



# Investigating the linkage between simulated precipitation climatology and ENSO-related precipitation anomaly based on multi-model and perturbed parameter ensembles

Ben Yang<sup>1</sup> · Yaocun Zhang<sup>1</sup> · Zhun Guo<sup>2</sup> · Yun Qian<sup>3</sup> · Anning Huang<sup>1</sup> · Yang Zhou<sup>4</sup>

Received: 8 May 2019 / Accepted: 26 August 2019  
© Springer-Verlag GmbH Austria, part of Springer Nature 2019

## Abstract

It remains a challenge for climate models to correctly capture the relationship between precipitation and ENSO. This study examines the linkage between the simulated precipitation climatology and ENSO-related precipitation anomaly during boreal winter based on the multi-model ensemble from the Atmospheric Model Intercomparison Project Phase 5 (AMIP5) and perturbed parameter ensemble (PPE) with the Beijing Climate Center (BCC) atmospheric model. The AMIP5 models have large biases in simulating the tropical precipitation anomaly during El Niño, such as the shifts of the Inter-Tropical Convergence Zone (ITCZ) and South Pacific Convergence Zone (SPCZ). The inter-model differences show that the precipitation change in response to sea surface temperature (SST) change increases with enhanced precipitation climatology. The ENSO-related precipitation anomaly can also be related to the spatial distribution of the mean-state precipitation. The simulated ITCZ/SPCZ displacements are significantly correlated with the spatial precipitation-SST relationship in the mean state. Models with stronger mean-state precipitation-SST relationship also produce stronger SPCZ/ITCZ displacements. The mean-state tropical precipitation also has strong impacts on the ENSO-related precipitation anomalies over East Asia. In the BCC PPE, the connection between the mean-state precipitation and ENSO-related precipitation anomaly is overall consistent with that in AMIP5. Parameters associated with the low-cloud and deep convection processes are the most influential ones for the precipitation simulations in BCC. Compared with the version in AMIP5, the new BCC model can better simulate the precipitation climatology and the relationship between ENSO and precipitation over southern China. These results have important implications for model development and model-based climate predictions.

## 1 Introduction

General circulation models (GCMs) have been widely applied in climate simulations, predictions, and projections. Although

GCMs are able to capture salient features in the climate system, different models often produce large spread in the projections of future climate at both regional and global scales (Cubasch et al. 2001; Jackson et al. 2008; Brown et al. 2012; Lee and Wang 2014; Lintner et al. 2016). The inter-model diversities are largely contributed by uncertainties in the representations of model dynamical cores, physical parameterizations, and tunable model parameters (Gilmore et al. 2004; Hou et al. 2012; Yang et al. 2013, 2015a; Zhao et al. 2013; Guo et al. 2014, 2015; Boyle et al. 2015; Qian et al. 2015; Posselt et al. 2016). Ensemble strategy by using multiple models or perturbed parameter values has been effectively applied to assess the model uncertainties of different sources (Giorgi and Mearns 2002; Lopez et al. 2006; Murphy et al. 2014; Collins et al. 2011; Hawkins and Sutton 2009; Yang et al. 2012; Yan et al. 2015).

Our confidence in the future climate projections highly relies on climate models' ability in reproducing current

✉ Ben Yang  
byang@nju.edu.cn

<sup>1</sup> CMA-NJU Joint Laboratory for Climate Prediction Studies and School of Atmospheric Sciences, Nanjing University, Nanjing, China

<sup>2</sup> State Key Laboratory of Numerical Modeling for Atmospheric Sciences and Geophysical Fluid Dynamics, Institute of Atmospheric Physics, Chinese Academy of Sciences, Beijing, China

<sup>3</sup> Pacific Northwest National Laboratory, Richland, WA, USA

<sup>4</sup> Collaborative Innovation Center on Forecast and Evaluation of Meteorological Disasters/Key Laboratory of Meteorological Disaster, Ministry of Education, Nanjing University of Information Science and Technology, Nanjing, China

climate (Grose et al. 2014; Li et al. 2017). Numerous efforts have been made by different individual institutes to improve the simulation of the mean-state climate (Watanabe et al. 2010; Hurrell et al. 2013; Wu et al. 2010; Hourdin et al. 2017). However, systematic limitations still exist in the current-generation GCMs, including those participating the Coupled Model Intercomparison Project Phase 5 (CMIP5) (Taylor et al. 2012). The majority of the CMIP5 models share many common biases, such as the double Inter-Tropical Convergence Zones (ITCZs), which are usually accompanied by a near-zonal orientation of the South Pacific Convergence Zone (SPCZ) (Brown et al. 2013; Li and Xie 2014). Most models still have difficulties in realistically simulating the East Asian summer monsoon rain belt (Huang et al. 2013; Sperber et al. 2013; Song and Zhou 2014b). In addition to the mean state, it is also important to validate the simulated climate variability (Vincent et al. 2011; Song and Zhou 2014a; Yang et al. 2015b), which is a key element for climate prediction and projection.

The El Niño–Southern Oscillation (ENSO) is the most significant interannual mode in the tropics and has pronounced impacts on the global climate system (Neelin et al. 1998; Wallace et al. 1998; McPhaden et al. 2006; Clarke 2008). Its sea surface temperature (SST) variations modulate the Walker circulation and tropical convection (Lindzen and Nigam 1987; Chung and Power 2015), which can further affect the climate over extratropical regions (Ropelewski and Halpert 1987; Wu and Wang 2002; Wang and Zhang 2002; Wang et al. 2000, 2008; Xie et al. 2009; He and Wang 2013; Zhou et al. 2014; Zhang et al. 2016; Yang et al. 2018). Many previous studies have investigated the atmospheric responses to ENSO simulated by different GCMs (Choi et al. 2015; Gong et al. 2015; Murphy et al. 2015). Compared with CMIP3, the CMIP5 coupled GCMs (CGCMs) can generally better reproduce the precipitation changes during El Niño, such as the displacements of precipitation over ITCZ and SPCZ (Brown et al. 2013; Bellenger et al. 2014; Kim et al. 2014; Ham and Kug 2015). However, the CMIP5 models still exhibit biases evident in the ENSO-related precipitation. For instance, the area with positive precipitation anomaly extends further west by about 20° relative to that in observation during El Niño (Kug et al. 2012; Zhang and Sun 2014; Ham and Kug 2015). In some CMIP5 models, the year-to-year meridional shift of SPCZ is remarkably underestimated (Brown et al. 2013). Such biases might affect the CGCM-based seasonal predictions (Yang et al. 2014; Li et al. 2016; Lu et al. 2017).

The climatological mean state can modulate the simulated climate variability to a large degree (e.g., Sperber and Palmer 1996; Kang et al. 2002; Zhang et al. 2012; Annamalai and Liu 2005; Watanabe et al. 2010; Brown et al. 2014; Ham and Kug 2014; Li et al. 2017). Using the Beijing Climate Center (BCC) atmospheric GCM (AGCM), Yang et al. (2015b) revealed a strong connection between the simulated mean state and

interannual variability of the Asian summer monsoon precipitation when key physical parameters were perturbed. Ham and Kug (2015) showed, that in the CMIP5 CGCMs, the ENSO-related precipitation simulation is related to the simulated mean state, with wetter climatology over the central Pacific leading to a west shift of the positive precipitation anomaly. Previous studies also revealed the strong effects of the mean bias of precipitation on future projections (Li et al. 2016a, b).

Previous studies have evaluated the ENSO-related precipitation simulations in both AGCMs and CGCMs (e.g., Zhang et al. 2012; Yang et al. 2015b; Ham and Kug 2015). However, the reasons for the bias in precipitation anomaly and its relationship with the simulated climatology are still unclear. Compared with AGCMs, the precipitation biases in CGCMs are strongly coupled with those in SST (Zhang and Sun 2014; Ham and Kug 2015; Dai and Arkin 2017), which introduces additional difficulties to understand those biases. In this study, simulations of 18 AGCMs from the Atmospheric Model Intercomparison Project Phase 5 (AMIP5; from CMIP5) are used to investigate whether the biases of the ENSO-related precipitation anomaly are related to the biases in the mean-state precipitation. Moreover, we apply the perturbed parameter ensemble (PPE) with the BCC AGCM to quantify the sensitivity of precipitation climatology and anomaly to different parameters associated with various physical processes, which can provide insights for further model development.

The model and observational datasets and applied methodology are described in Section 2. In Section 3, we use the multi-model ensemble from AMIP5 and PPE using the BCC AGCM to examine the connection between the simulated precipitation climatology and ENSO-related precipitation anomaly during boreal winter when El Niño is at its peak phase. Results show that the simulated precipitation anomaly can be related to the mean-state precipitation in terms of both magnitude and spatial characteristics. A summary is given in Section 4 along with discussions.

## 2 Models and datasets

### 2.1 Observations

We use the monthly precipitation data from two satellite products, i.e., the Global Precipitation Climatology Project (GPCP) (Adler et al. 2003) and Climate Prediction Center Merged Analysis of Precipitation (CMAP) (Xie and Arkin 1997), to evaluate the simulated precipitation climatology and ENSO-related precipitation anomaly. The two datasets have a grid spacing of 2.5°. The datasets can be freely downloaded from <https://www.esrl.noaa.gov/psd/data/gridded/data.gpcp.html>. Monthly SST fields are derived from the Hadley Centre Sea Ice and Sea Surface

Temperature data set (HadISST) version 1.1 at 1° resolution (available at: <https://www.metoffice.gov.uk/hadobs/hadisst/>).

## 2.2 AMIP5 models

The simulated precipitation data from 18 AMIP5 models are applied in this study (<https://esgf-node.llnl.gov/projects/esgf-llnl/>; Taylor et al. 2012). Precipitation climatology and ENSO-related precipitation anomaly during boreal winter are calculated based on the results of 1980–2004 from the first member of each model. Detailed information of the used AMIP5 models is given in Table 1. For each year, boreal winter means December of that year and January–February of the next year (i.e., December–January–February, DJF). The Niño index is defined as the 3-month running mean of SST anomalies in the Niño 3.4 region (i.e., 5°N–5°S, 120°–170°W), ([http://origin.cpc.ncep.noaa.gov/products/analysis\\_monitoring/ensostuff/ONI\\_v5.php](http://origin.cpc.ncep.noaa.gov/products/analysis_monitoring/ensostuff/ONI_v5.php)). Years with the Niño index above + 0.5 °C in DJF are identified as El Niño years. During the analysis period, there are seven El Niño years, i.e., 1982, 1987, 1991, 1994, 1997, 2002, and 2004. Here, the ENSO-related anomaly (e.g., in precipitation or SST) means the average of anomalies in all the El Niño years within the analyses period.

## 2.3 BCC PPE experiments

In addition to the AMIP5 results, we also examine the connection between the simulated precipitation climatology and

precipitation anomaly in the PPE using the atmospheric model of BCC-CSM1.1 m (Wu et al. 2010), which is among the AMIP5 models applied in this study (Table 1). We explore the sensitivity of precipitation to eight physical parameters associated with the cloud and precipitation processes (Table 2). A hundred parameter sets were generated by the Latin hypercube sampling method (McKay et al. 1979; Stein 1987), and each set was employed to conduct the BCC AGCM experiment from January 1, 2000, to December 31, 2008, with the first half year discarded as spin-up. Thus, a total of 100 experiments covering 8 boreal winters (i.e., 2000–2007) are available for the sensitivity analysis, with three winters in El Niño years (i.e., 2002, 2004, and 2006). For more details about the model configuration and parameter sampling, please refer to Yang et al. (2015b).

## 3 Results

### 3.1 Precipitation simulation in AMIP5

#### 3.1.1 Spatial patterns of precipitation climatology and anomaly

The AMIP5 models with prescribed SST can generally capture the observed precipitation pattern in DJF in terms of both climatology and ENSO-related anomaly (Fig. 1). High SSTs (i.e., above 29 °C) in the mean state (Fig. 1a) are mainly

**Table 1** Model names and host institutions of AMIP5 models used in this study

Model	Institute
ACCESS1.0	Commonwealth Scientific and Industrial Research Organisation and Bureau of Meteorology, Australia
CCSM4	National Center for Atmospheric Research, USA
CESM1-CAM5	National Center for Atmospheric Research, USA
CMCC-CM	Centro Euro-Mediterraneo per I Cambiamenti Climatici, Italy
CNRM-CM5	Centre National de Recherches Meteorologiques/Centre Europeen de Recherche et Formation Avancees en Calcul Scientifique, France
CSIRO-Mk3.6	Commonwealth Scientific and Industrial Research Organisation, Australia
FGOALS-g2	LASG, Institute of Atmospheric Physics, Chinese Academy of Sciences; and CESS, Tsinghua University, China
FGOALS-s2	LASG, Institute of Atmospheric Physics, Chinese Academy of Sciences, China
GFDL-CM3	Geophysical Fluid Dynamics Laboratory, USA
GISS-E2-R	NASA Goddard Institute for Space Studies, U
HadGEM2-A	Met Office Hadley Centre, UK
INM-CM4	Institute for Numerical Mathematics, Russia
IPSL-CM5A-MR	Institut Pierre-Simon Laplace, France
MIROC5	Atmosphere and Ocean Research Institute (The University of Tokyo), National Institute for Environmental Studies, and Japan Agency for Marine-Earth Science and Technology, Japan
MPI-ESM-LR	Max Planck Institute for Meteorology, Germany
MPI-ESM-MR	Max Planck Institute for Meteorology, Germany
BCC_CSM1.1	Beijing Climate Center, China Meteorological Administration, China
BCC_CSM1.1 m	Beijing Climate Center, China Meteorological Administration, China

**Table 2** Descriptions and investigated ranges of parameters in BCC-CSM1.1 m AGCM

Parameter	Description	Default	Range
$Q_{ic}$	Autoconversion size threshold for ice (m)	$4 \times 10^{-4}$	$[1 \times 10^{-4}, 5 \times 10^{-4}]$
$K_{e\_strat}$	Evaporation efficiency for stratiform precipitation $[(\text{kg m}^{-2} \text{s}^{-1})^{-1/2} \text{s}^{-1}]$	$3 \times 10^{-6}$	$[1 \times 10^{-6}, 20 \times 10^{-6}]$
$RH_{low}$	Threshold RH for low stable clouds (-)	0.9	[0.8, 0.99]
$RH_{high}$	Threshold RH for high stable clouds (-)	0.65	[0.65, 0.85]
$C_{0\_shal}$	Precipitation efficiency for shallow convection ( $\text{m}^{-1}$ )	$0.8 \times 10^{-4}$	$[0.5 \times 10^{-4}, 3 \times 10^{-4}]$
$C_{0\_deep}$	Precipitation efficiency for deep convection ( $\text{m}^{-1}$ )	$3 \times 10^{-3}$	$[1 \times 10^{-3}, 6 \times 10^{-3}]$
$K_{e\_conv}$	Evaporation efficiency for deep convective precipitation $[(\text{kg m}^{-2} \text{s}^{-1})^{-1/2} \text{s}^{-1}]$	$1 \times 10^{-6}$	$[0.5 \times 10^{-6}, 10 \times 10^{-6}]$
$\beta$	Downdraft coefficient for deep convection (-)	2	[1, 3]

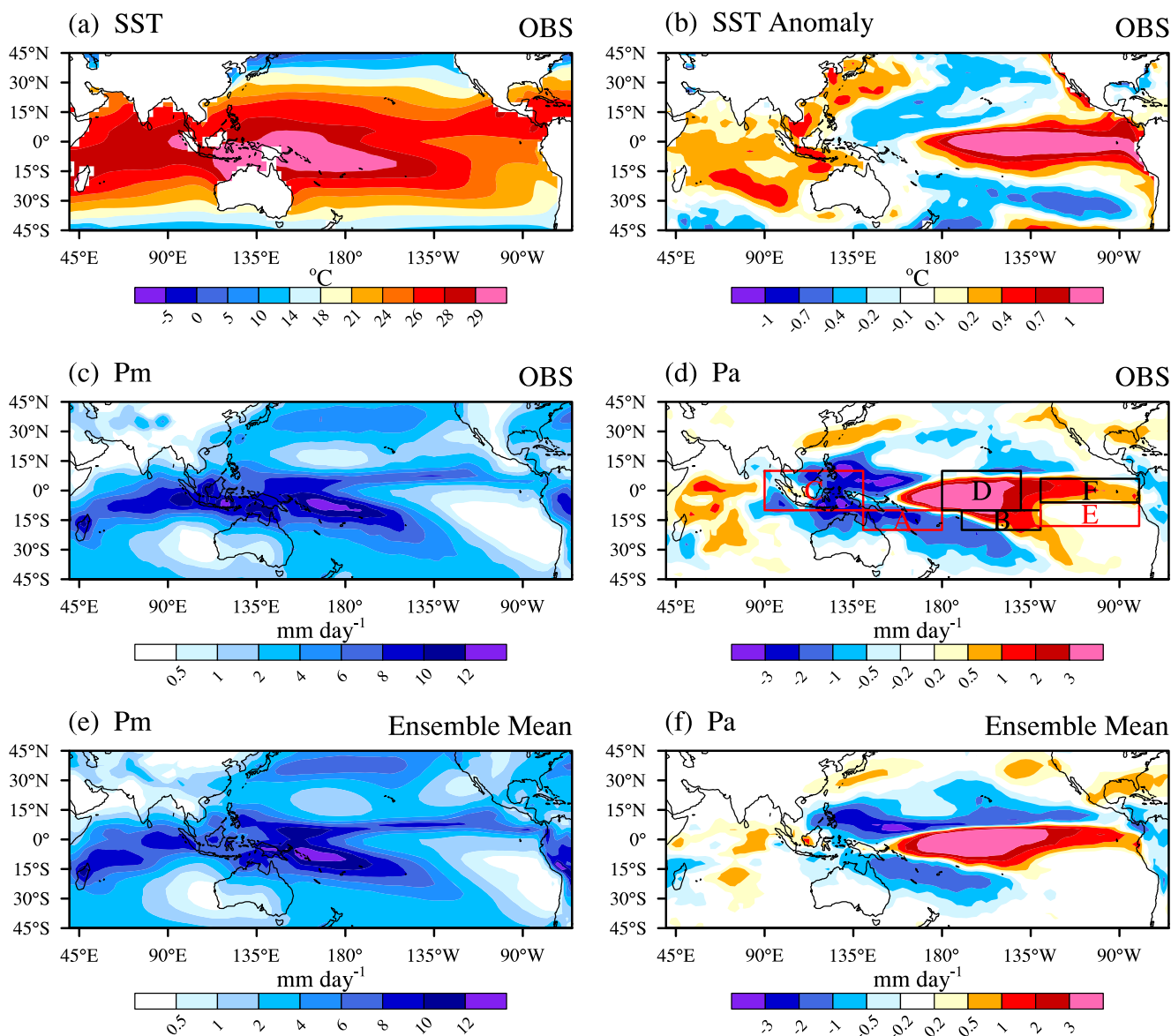


**Fig. 1** Spatial distributions of **a, c** climatological mean states and **b, d** ENSO-related anomalies (defined in Section 2.2) for **a, b** SST and **c, d** precipitation during DJF (1980–2004) from observation

(HadISST&CMAP). Climatological mean precipitation and ENSO-related precipitation anomalies from ensemble mean of the 18 AMIP5 models are shown in **e** and **f**, respectively

located over the equatorial western Pacific (EWP) and oceans around the Maritime Continent. Areas with warm surface extend southeastward to the southern Pacific. The precipitation pattern in observation (Fig. 1c) is consistent with the SST pattern, with strong rainfall over ITCZ, SPCZ, and the tropical Indian Ocean. The SST distribution during El Niño (Fig. 1b) features above-normal values over the equatorial central and eastern Pacific (ECP and EEP, respectively) and below-normal values over EWP and the mid-latitude Pacific. Increased SST is also seen over the tropical Indian Ocean. Correspondingly, precipitation is increased over ECP and EEP but decreased to the west during El Niño (Fig. 1d). The precipitation response indicates a shift of strong rainfall center from west to east in ITCZ (e.g., Ham and Kug 2015). The SPCZ rainfall exhibits a northeastward movement during El Niño (e.g., Vincent et al. 2011). Although the AMIP5 ensemble-mean results can generally reproduce the precipitation climatology and anomaly (Fig. 1e, f), evident biases can still be seen, such as that in the mean-state SPCZ distribution (Fig. 1c vs. Fig. 1e). The simulated precipitation responses during El Niño are too weak over the Maritime Continent and tropical Indian Ocean (Fig. 1d vs. Fig. 1f).

We further compare the simulated precipitation anomalies in each of the AMIP5 models against observation (Fig. 2). The different models share some common biases although their results are different in many aspects. Nearly all the models produce positive biases of precipitation anomalies over the Maritime Continent. Large errors exist in SPCZ but with different individual models having their own bias patterns, indicating a large inter-model spread in the representation of the SPCZ shift during El Niño.

### 3.1.2 Linkage between precipitation climatology and anomaly

Previous studies have revealed that the climatological mean state can modulate the simulated climate variability to a large degree (e.g., Sperber and Palmer 1996; Kang et al. 2002; Zhang et al. 2012; Brown et al. 2014; Ham and Kug 2014). Figure 3 shows the spatial pattern of the relationship (at each grid point) between the simulated precipitation anomaly and precipitation climatology (i.e. regression coefficient between them) among different AMIP5 models. Apparently, except for over the Maritime Continent, the regression pattern largely resembles that of SST anomaly (Fig. 1b). Thus, the positive (negative) precipitation anomaly in response to positive (negative) SST anomaly increases with enhanced precipitation climatology, suggesting that the latter is contributed mostly by the increased rainfall in wet years, which amplifies the discrepancy among different years.

The ENSO-related precipitation anomaly could also be, at least in part, related to the spatial distribution of the mean-state precipitation because both of them can be explained by the

changes in SST. As shown in Fig. 1, the shifts in SPCZ and ITCZ during El Niño closely follow the movement of high SSTs. Here, we use the difference of precipitation anomalies between region B and region A (representing the eastern and western SPCZ, respectively, Fig. 1d) to define the extent of the SPCZ displacement. The spatial precipitation-SST relationship in the mean state is loosely calculated as the regression of precipitation against SST over a limited region covering SPCZ (i.e., 30°S–20°N and 120°E–140°W with SST above 27 °C). The SPCZ displacement and mean-state precipitation-SST relationship in different models are compared (Fig. 4(a)). As shown, the two aspects are strongly interrelated among different models (colored markers), with a correlation coefficient of 0.86 that is statistically significant at 99% confidence level. The biases in the mean-state precipitation-SST relationship well correspond to the biases in the SPCZ displacement, despite the uncertainty in the two observational datasets (black markers). For example, all the models with an underestimated mean-state relationship (markers in the left-bottom corner in Fig. 4(a)) produce a too weak SPCZ displacement, which can also be seen in Fig. 2. On the contrary, the two models (BCC-CSM1.1 and FGOALS-g2) with an overestimated mean-state relationship produce a too strong shift of SPCZ. Those models with relatively small biases in the mean-state relationship show a comparable extent of the SPCZ displacement with that in observation.

Similar analyses can be applied for the movement of ITCZ (Fig. 4(b), (c)). Here, we use the difference of precipitation anomalies between region D (F) and region C (E) to represent the eastward displacement of ITCZ (equatorward displacement of ITCZ over the eastern Pacific). Note that the spatial precipitation-SST relationships in the mean state are based on different regions (see the caption of Fig. 4) from that for the SPCZ analysis. Both the eastward and equatorward displacements of ITCZ are highly related to the mean-state precipitation-SST relationship. Many models overestimate the equatorward displacement of ITCZ (Fig. 4(c)), corresponding to the overestimated mean-state relationship. Regarding the eastward displacement of ITCZ, there exists a large uncertainty in the observations (Fig. 4(b)). However, this does not affect the inter-model relationship; the correlation between the mean-state relationship and the eastward displacement of ITCZ is statistically significant at 99% confidence level. Similar results can be found when focusing on the relationship between precipitation anomaly and precipitation climatology for each individual El Niño year (not shown).

### 3.1.3 Precipitation anomalies over East Asia and North America

As revealed by previous studies (Wang et al. 2000; Yang et al. 2018; Zhou et al. 2014), ENSO has a significant impact on the precipitation over East Asia and North America. The 18

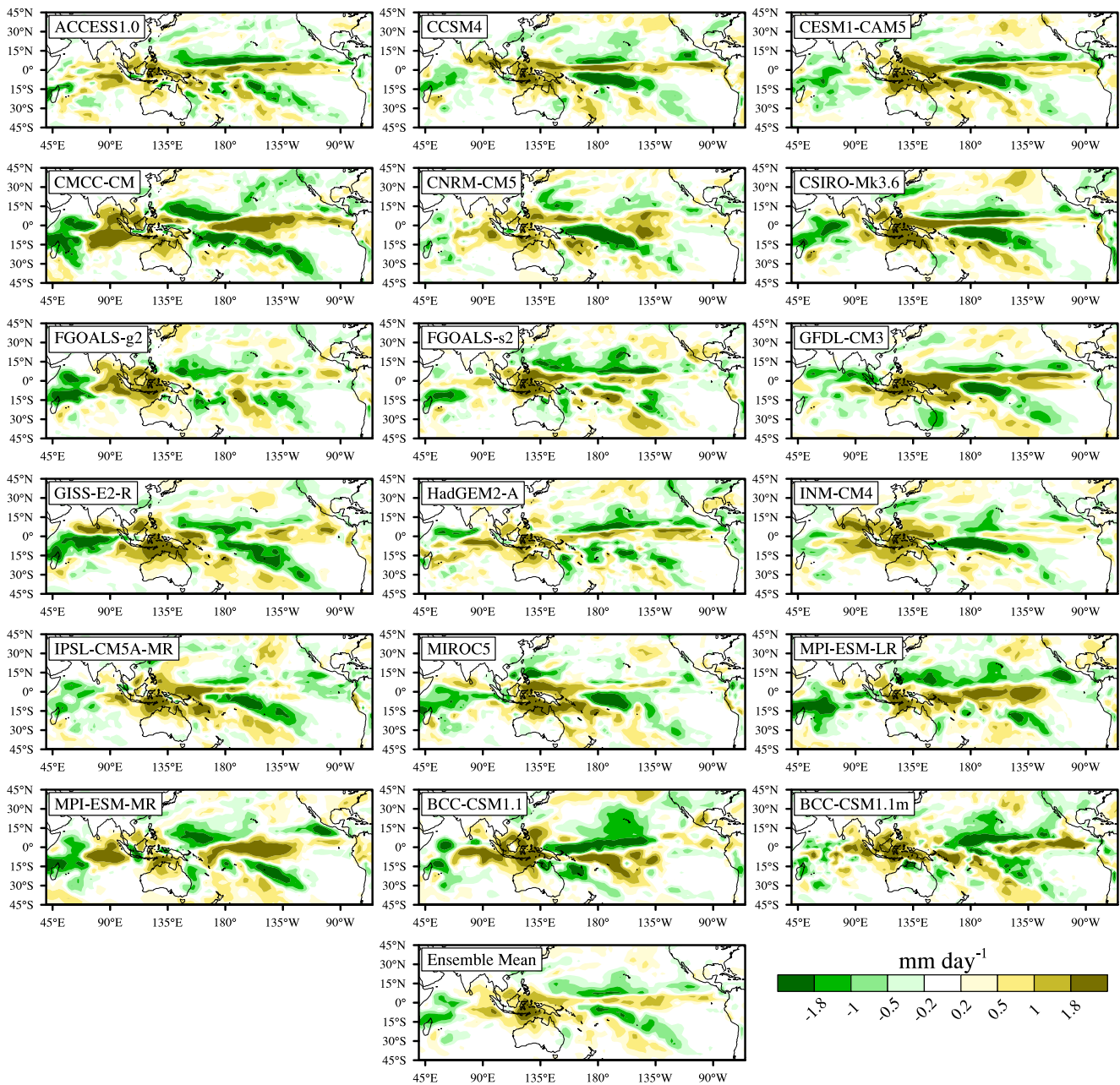
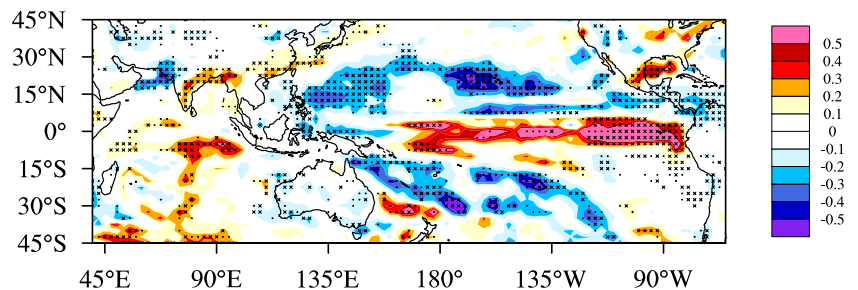


**Fig. 2** Spatial distributions of simulated biases (relative to CMAP precipitation) of ENSO-related precipitation anomalies during DJF (1980–2004) in each of the AMIP5 models and their ensemble mean

models are classified into three groups (each group with 6 members) based on their skills in simulating the mean-state

spatial pattern of precipitation over the tropical Pacific, and the spatial patterns of ENSO-related precipitation anomalies

**Fig. 3** Spatial distribution of ENSO-related precipitation anomaly regressed against precipitation climatology across model members in AMIP5. Areas where the relationship is statistically significant at 95% (90%) confidence level are masked by crosses (dots)



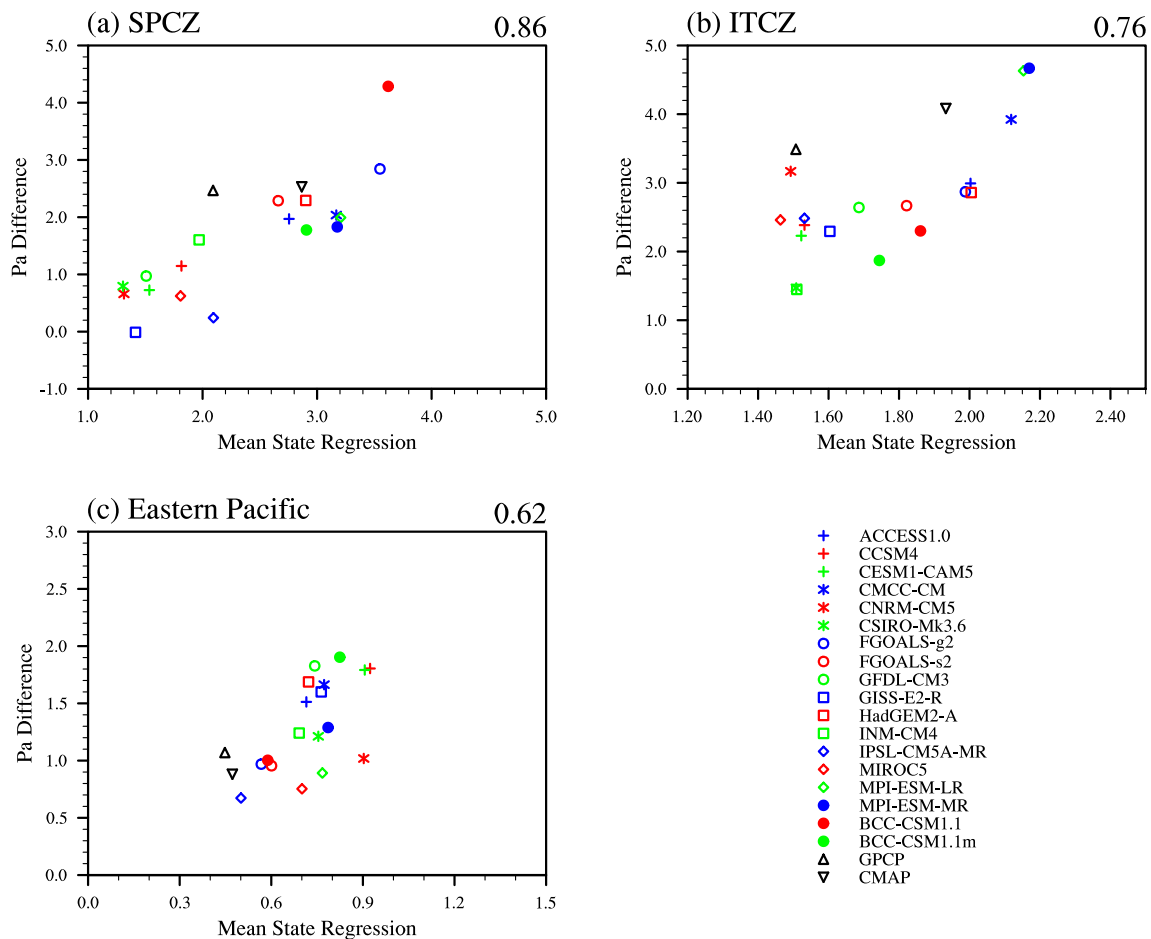


**Fig. 4** Scatter plots for spatial precipitation–SST relationship in the mean state ( $x$ -axis) vs. ENSO-related displacement ( $y$ -axis) in (a) SPCZ and (b, c) ITCZ (b: eastward displacement; c: equatorward displacement) during DJF (1980–2004) in observations (black markers) and different AMIP5 models (colored markers). The mean-state spatial precipitation–SST relationship is represented by the regression of precipitation against SST ( $\text{mm day}^{-1} \text{ } ^\circ\text{C}^{-1}$ ) over oceans with SST above  $27 \text{ } ^\circ\text{C}$  in  $30^\circ\text{S}$ – $20^\circ\text{N}$  and

$120^\circ\text{E}$ – $140^\circ\text{W}$  in (a), above  $25 \text{ } ^\circ\text{C}$  in  $30^\circ\text{S}$ – $20^\circ\text{N}$  and  $50^\circ\text{E}$ – $100^\circ\text{W}$  in (b), and above  $20 \text{ } ^\circ\text{C}$  in  $30^\circ\text{S}$ – $20^\circ\text{N}$  and  $130^\circ\text{W}$ – $80^\circ\text{W}$  in (c). The displacements in precipitation ( $\text{mm day}^{-1}$ ) in (a), (b), and (c) are defined as the difference in precipitation anomalies between regions B and A, D and C, and F and E (see Fig. 1d), respectively. In each panel, the correlation coefficient between the two variables is given at the top-right corner

averaged in the first (i.e., low-skill) and third (i.e., high-skill) groups are given in Fig. 5. Compared with observation (Fig. 1d), the low-skill models underestimate and overestimate the precipitation anomalies over land regions in East Asia and North America, respectively (Fig. 5(a)). In contrast, the models with improved mean-state precipitation agree more with observation in terms of the precipitation anomalies over these land regions (Fig. 5(b)). Further analyses indicate that the model skills in simulating the interannual variation of wintertime precipitation over southern China (i.e., temporal correlation coefficient between simulation and observation) are positively correlated (statistically significant at 95% confidence level) with the model skills in simulating the mean-state tropical precipitation (Fig. 6). Note that the East Asian precipitation during winter can be strongly modulated by the simulated subtropical jet stream (Huang et al. 2019; Seager et al. 2005; Yang et al. 2019), which might also be sensitive to the precipitation simulation in the tropics.

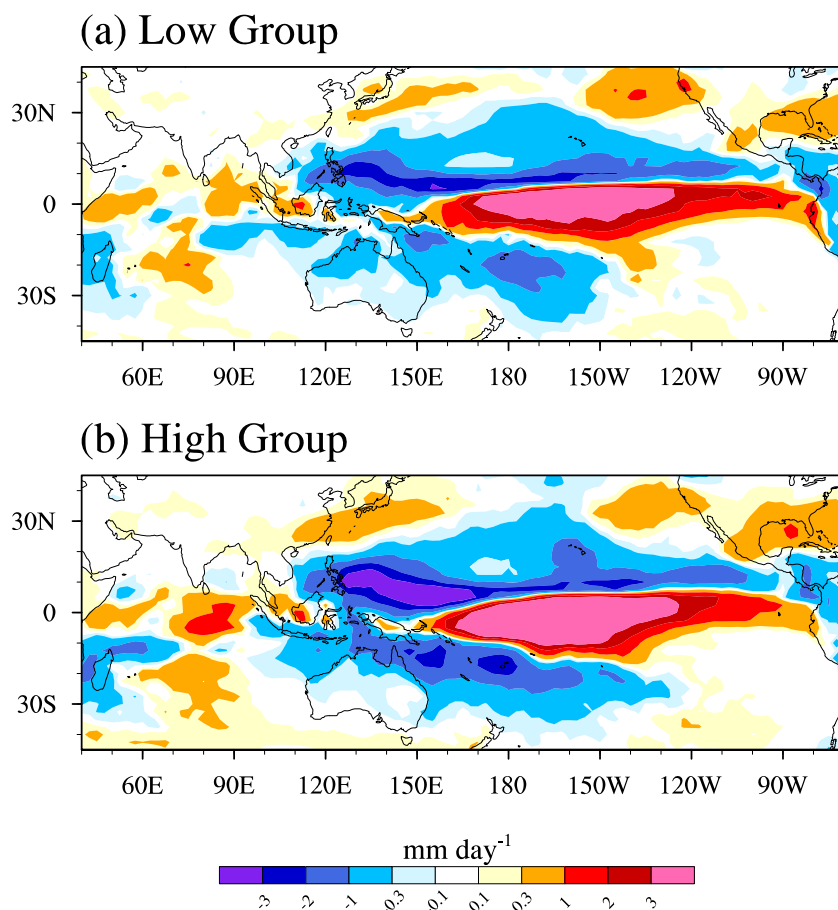
## 3.2 Precipitation climatology and anomaly in BCC PPE

### 3.2.1 Parameter impacts on precipitation simulation

The precipitation differences among different AMIP5 members can be attributed to their discrepancies in dynamical cores, resolutions, and physical parameterizations. In addition, parameter uncertainty in each individual model may also be important for the simulated precipitation climatology and anomaly (Yang et al. 2015b). In this section, we examine whether the above relationship between the simulated precipitation climatology and anomaly still exists in the PPE simulations using the BCC AGCM (i.e. atmospheric component of BCC-CSM1.1 m), and which processes are important for such relationship.

Compared with during 1980–2004 (Fig. 1b), the ENSO-related SST pattern during 2000–2007 is more like a Centre-Pacific El Niño type (Fig. 7a). The precipitation anomaly and

**Fig. 5** Spatial distributions of ENSO-related precipitation anomalies from ensemble mean of the six models with the (a) lowest and (b) highest skills in simulating the mean-state spatial pattern of precipitation over the tropical Pacific (30°S–20°N and 135°E–105°W)



mean-state precipitation magnitude are significantly positively correlated over ECP (Fig. 7b), indicating that over areas with positive SST anomaly, the increased precipitation

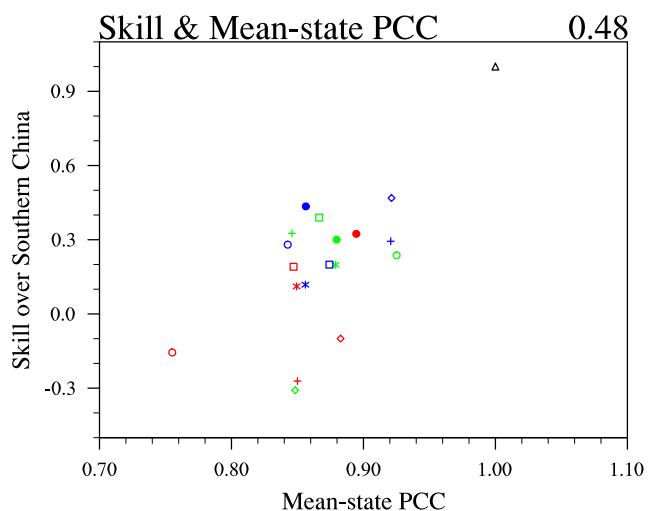


**Fig. 6** Scatter plots for model skills in simulating the mean-state spatial pattern of precipitation over the tropical Pacific (x-axis) vs. model skills in simulating the interannual variation of precipitation over southern China (21°N–30°N and 110°E–123°W) during DJF (1980–2004). The correlation coefficient between the two skills is given at the top-right corner

anomaly corresponds to enhanced precipitation climatology. The precipitation climatology and precipitation anomaly are negatively correlated over NWP, SPCZ, and higher-latitude regions in the Pacific, corresponding to the negative SST anomaly there. These results suggest that the precipitation changes due to parameter tuning in BCC are more evident in wet years than in dry years, which is similar to the AMIP5 results (Fig. 3).

However, different from that in AMIP5, the correlation between precipitation anomaly and the spatial precipitation-SST relationship in the mean state is weak in the BCC PPE (Fig. 8 vs. Fig. 4). The values of each parameter are used to split the 100 PPE members into five groups, and the differences between the fifth (i.e., high-value of parameter) and first (low-value of parameter) groups represent the main effects of that parameter. The most influential parameters for precipitation simulations are *RH\_low* (red markers in Fig. 8(a)) or *Ke\_conv* (green markers in Fig. 8(a)) lead to stronger mean-state precipitation-SST relationship and intensified SPCZ displacement. Differently, larger values of *C<sub>o\_deep</sub>* (blue markers) cause stronger mean-state

**Fig. 7** **a** ENSO-related SST anomalies from 2000 to 2007. **b** Same as Fig. 3 but for the results from 2000 to 2007 in the BCC PPE

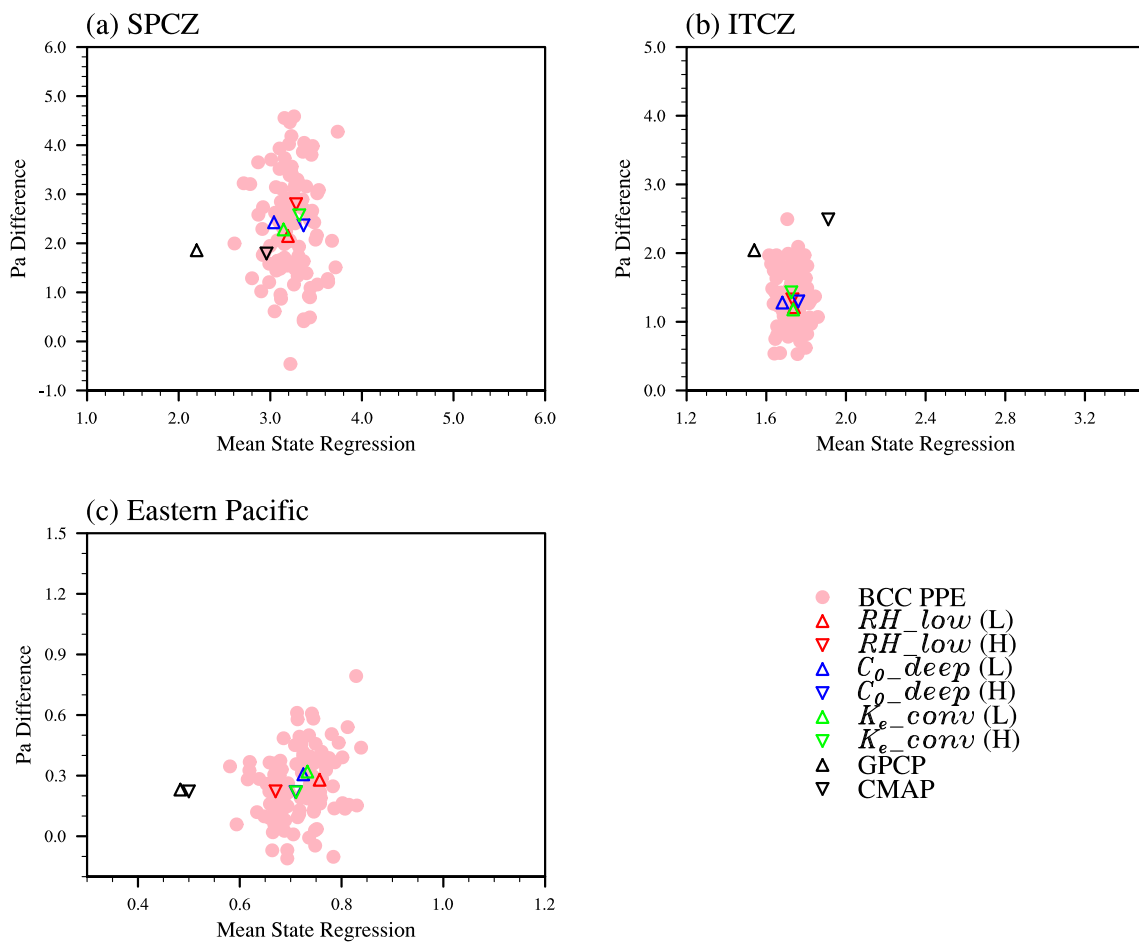
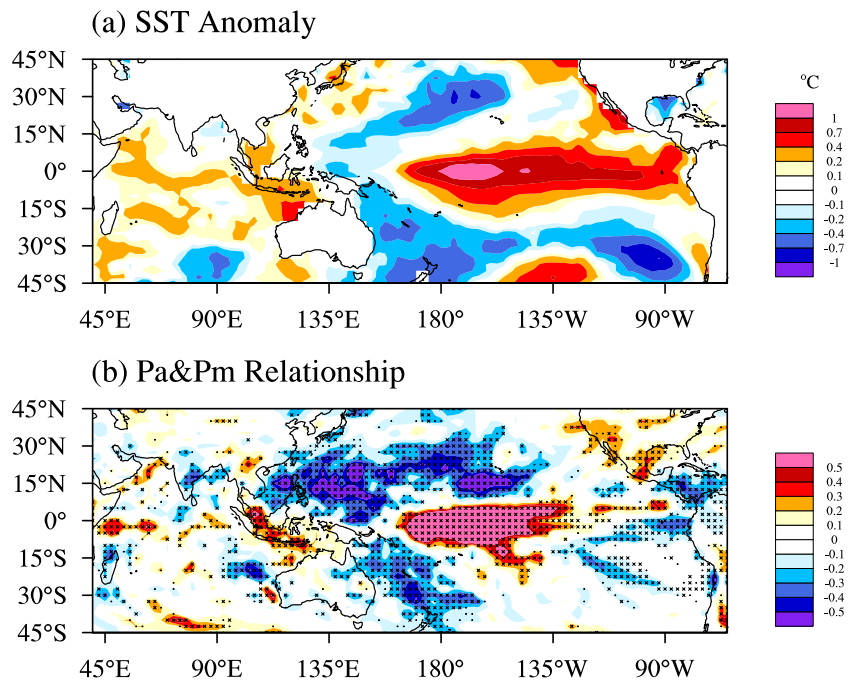


**Fig. 8** Same as Fig. 4 but for the results using BCC PPE from 2000 to 2007. The triangle markers in each panel represent the averages from the experiments with low (L) and high (H) values of three influential parameters indicated in the bottom-right corner

relationship but slightly weakened SPCZ displacement. These contrasting effects partly explain the weak correlation between the precipitation anomaly and mean-state relationship when simultaneously perturbing multiple parameters. The correlation between the precipitation anomaly and mean-state relationship is also weak for the movement of ITCZ (Fig. 8(b), (c)).

To understand the “conflicting” results in AMIP5 and in the BCC PPE, we further explore the spatial characteristics of the impacts of the above three parameters on precipitation (Fig. 9). We find that increasing the value of  $RH_{low}$  leads to decreases in the mean-state precipitation over most areas (Fig. 9(a)) except for over SPCZ. This is because larger  $RH_{low}$  suppresses the stratiform process (Qian et al. 2015) but might enhance deep convection in particular regions. Larger values of  $C_{o\_deep}$  and  $Ke_{conv}$  indicate stronger rain generation and evaporation, respectively, which should have opposite effects on the precipitation magnitude. However, the mean-state precipitation exhibits similar responses to these two parameters (Fig. 9(d), (g)). This is likely because their impacts are respectively more important over wet and dry regions (Yang et al. 2015a), leading to similar teleconnection patterns in the tropics (Yang et al. 2015b). Larger  $RH_{low}$  or  $Ke_{conv}$  results in increased precipitation anomaly over the eastern SPCZ (i.e., intensified SPCZ displacement; Fig. 9(b), (h)), corresponding to the intensified SPCZ and stronger spatial precipitation-SST relationship in the mean state. The impact of  $C_{o\_deep}$  on precipitation anomaly is more complicated

(Fig. 9(e)). When focusing on each individual parameter, the relationships between the precipitation climatology and precipitation anomaly (right panels in Fig. 9) are overall consistent with that based on all the PPE members (Fig. 7b).

We can see that the sensitivities of the mean-state precipitation to parameters exhibit high space dependence (left panels in Fig. 9). In ITCZ, larger  $RH_{low}$  leads to reduced precipitation and thus weakened spatial precipitation-SST relationship there as well. Meanwhile, in SPCZ, the precipitation-SST relationship is stronger, which is associated with the enhanced precipitation magnitude. As a result, the changes in the mean-state precipitation-SST relationship are small when averaged over a very large domain (see Fig. 8), which is different from that in AMIP5. Based on the BCC PPE experiments, we calculate the spatial precipitation-SST relationship in the mean state over a relatively smaller area (i.e., running region) centered at each grid point (Fig. 10a). We can find that over most areas in the tropics, the precipitation change due to SST anomaly is highly correlated with the spatial precipitation-SST relationship in the mean state, which is overall consistent with the results in AMIP5 (Fig. 10b). We find changing the scope of running region has only a very weak impact on the results.

### 3.2.2 Precipitation simulation in updated BCC model

As shown earlier, the standard BCC-CSM1.1 m has difficulties in realistically simulating the precipitation anomaly during

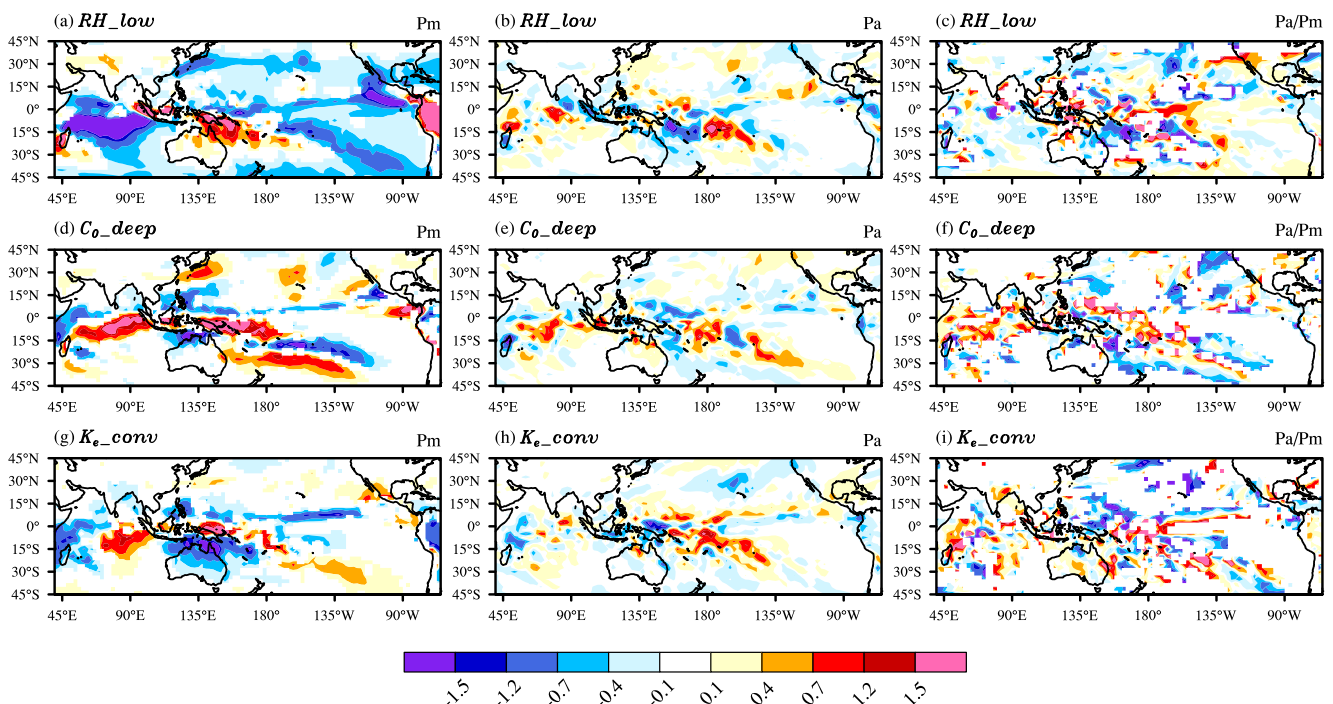
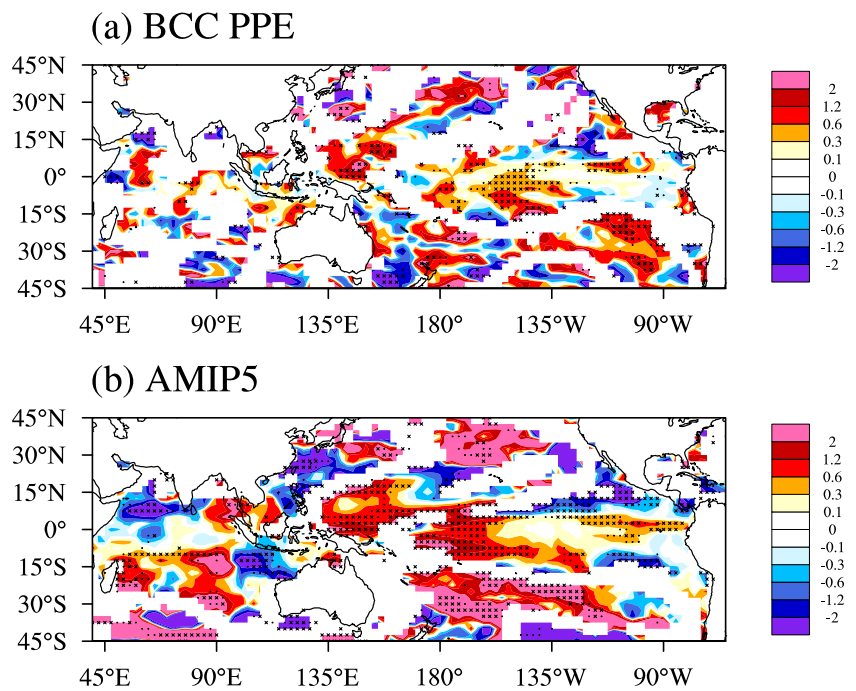


**Fig. 9** Sensitivities of (a, d, g) precipitation climatology ( $\text{mm day}^{-1}$ ) and (b, e, h) ENSO-related precipitation anomaly ( $\text{mm day}^{-1}$ ), as well as (c, f, i) their ratio (i.e., anomaly divided by climatology) to the parameters (a–c)

$RH_{low}$ , (d–f)  $C_{o\_deep}$ , and (g–i)  $Ke_{conv}$ . Areas with the response of precipitation climatology below  $0.1 \text{ mm day}^{-1}$  are masked out in (c, f, i)

**Fig. 10** Spatial distribution of the ENSO-related precipitation sensitivity (i.e., precipitation anomaly divided by SST anomaly) regressed on the mean-state spatial precipitation-SST relationship across members in the **a** BCC PPE and **b** AMIP5. The mean-state relationship is calculated based on the results within a  $7.5^\circ$  (in latitude)  $\times$   $275^\circ$  (in longitude) running region centered at each point. Areas masked by crosses (dots) indicate that the correlation between precipitation anomaly and mean-state relationship is statistically significant at 95% (90%) confidence level. Areas with the SST anomaly below  $0.1^\circ\text{C}$  are masked out



El Niño (Figs. 2 and 4). During the past several years, the BCC model has been updated for participating the upcoming CMIP6 (AMIP6) project. Several new features including the re-estimated physical parameter values (Yang et al. 2015b; Wu et al. 2019) have been implemented in the updated model. Currently, the model has three sub-versions with different horizontal resolutions, i.e., BCC-CSM2-LR, BCC-CSM2-MR, and BCC-CSM2-HR. The resolutions applied in the former two are corresponding to that in BCC-CSM1.1 and BCC-CSM1.1 m in AMIP5, respectively.

In BCC-CSM2-MR, the simulated precipitation climatology is remarkably improved compared with that in BCC-CSM1.1 m (Fig. 11). For example, the underestimated precipitation over the Maritime Continent and northwestern Pacific, as well as the overestimated precipitation over EEP and the western Indian Ocean in BCC-CSM1.1 m (Fig. 11a), has been mitigated in BCC-CSM2-MR (Fig. 11b vs. Fig. 11a). The updated model can also better simulate the impacts of ENSO on the interannual variation of precipitation over southern China (Fig. 12). In observation (Fig. 12a), precipitation over

**Fig. 11** Spatial distributions of climatological mean precipitation during DJF (1980-2004) from **a** BCC-CSM1.1 m minus observation (i.e., CMAP) and **b** BCC-CSM2-MR minus BCC-CSM1.1 m

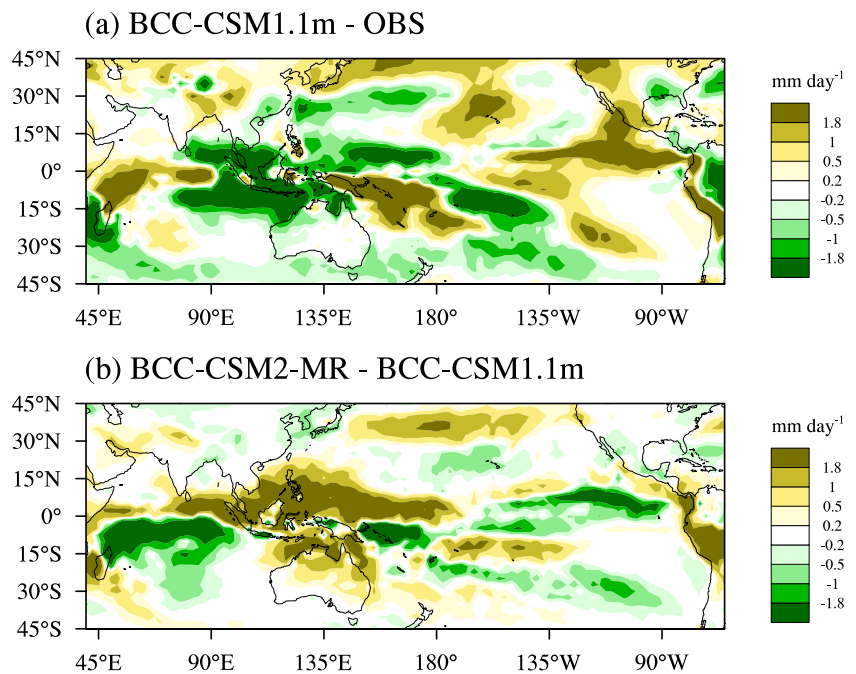
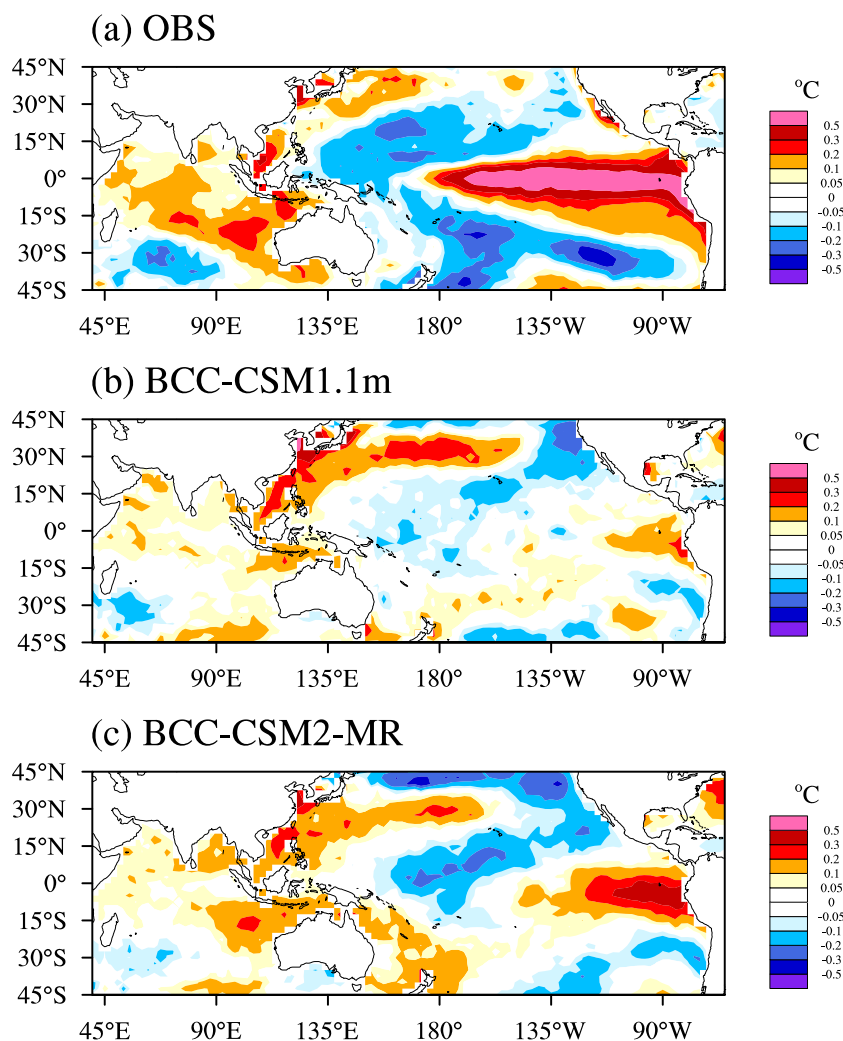


**Fig. 12** Spatial distributions of SST regressed on the DJF precipitation over southern China across years from 1980 to 2004 in **a** observation, **b** BCC-CSM1.1 m, and **c** BCC-CSM2-MR



southern China has a strong relationship with SST over EEP and ECP. Such relationship is largely underestimated in BCC-CSM1.1 m (Fig. 12b). Similar bias pattern can also be seen in the current BCC dynamical prediction system based on the coupled version of BCC-CSM1.1 m (Lu et al. 2017), highlighting the importance of improving the atmosphere model for climate predictions using coupled models. In contrast to BCC-CSM1.1 m, the updated model can better capture the remote connection between precipitation and SST (Fig. 12c).

#### 4 Summary and discussions

In this study, we investigated the linkage between the simulated precipitation climatology and ENSO-related precipitation anomaly during boreal winter. Experiments from two ensembles, i.e., the AMIP5 multi-model ensemble and the BCC AGCM PPE, were used for the analyses.

During El Niño, forced by the anomalous SST, ITCZ shifts eastward and equatorward and SPCZ shifts northeastward. The AMIP5 models can generally capture the observed precipitation pattern in terms of both climatology and ENSO-related anomaly. However, the models still have evident biases, such as the too weak precipitation anomalies over the Maritime Continent and tropical Indian Ocean during El Niño. The inter-model differences suggest that for most areas, the positive (negative) precipitation anomaly in response to positive (negative) SST anomaly increases with enhanced precipitation climatology. This implies that the increased mean-state precipitation is mostly contributed by the increased rainfall in wet years with above-normal SST, which amplifies the discrepancy between wet and dry years.

The ENSO-related precipitation anomaly could also be related to the spatial distribution of the mean-state precipitation because both of them can be explained by the changes in SST. As the results show, the SPCZ displacement and the spatial precipitation-SST relationship in the mean state are strongly interrelated among different models, with a correlation

coefficient of 0.86 between them that is statistically significant at 99% confidence level. Moreover, the bias in the mean-state precipitation-SST relationship corresponds well to the bias in the SPCZ displacement, i.e., the models with underestimated (overestimated) mean-state relationship also underestimate (overestimate) the SPCZ displacement. The simulated ITCZ displacement is also highly correlated with the simulated spatial precipitation-SST relationship in the mean state.

The simulations of the ENSO-related precipitation anomalies over East Asia are also related to the simulated mean-state tropical precipitation. The model skills in simulating the inter-annual variation of wintertime precipitation over southern China are significantly dependent on the simulated mean-state tropical precipitation.

Parameter uncertainties are important for precipitation simulations in each individual model. In the BCC PPE, the precipitation anomaly and precipitation climatology are significantly positively (negatively) correlated with each other over areas with positive (negative) SST anomaly. This suggests that the precipitation changes due to parameter tuning in BCC are more evident in wet years than in dry years, which is consistent with the AMIP5 results. The mean-state precipitation in BCC is mostly sensitive to the parameters associated with low-cloud and deep convection processes, but other processes such as those associated with boundary-layer mixing might also be important, which are not investigated here. Similar to the AMIP5 results, the ENSO-related precipitation anomaly is highly related to the spatial precipitation-SST relationship in the mean state. During the past several years, the BCC model has been updated including using the re-estimated physical parameter values. Compared with the version in AMIP5, the new BCC model can better simulate the precipitation climatology and the relationship between ENSO and precipitation over southern China.

This study reveals the strong connection between the ENSO-related precipitation anomaly and the mean-state precipitation magnitude and spatial pattern, which has important implications for simultaneously improving the climate mean state and variability simulations and for climate predictions based on dynamical model systems. However, given the large uncertainty in observation, more reliable datasets or metrics are needed for quantitatively evaluating the model results. This study mainly focuses on the AGCM results. When coupled to ocean models, the intrinsic biases of AGCMs can influence the simulated ocean features that can in turn affect the atmospheric responses, which deserves further investigations.

**Acknowledgments** We thank three anonymous reviewers for their careful reviews and constructive comments.

**Funding information** This study is jointly supported by the National Key R&D Program of China (Grant No. 2016YFA0602100) and the National

Natural Science Foundation of China (41675101). Yun Qian in this study is supported by the U.S. Department of Energy's Office of Science as part of the Atmospheric System Research (ASR) program. The Pacific Northwest National Laboratory is operated for DOE by Battelle Memorial Institute under contract DE-AC05-76RL01830. All the graphics in this study are created by the NCAR Command Language (NCL; doi:10.5065/D6WD3XH5).

## References

- Adler RF et al (2003) The version-2 global precipitation climatology project (GPCP) monthly precipitation analysis (1979-present). *J Hydrometeorol* 4:1147–1167
- Annamalai H, Liu P (2005) Response of the Asian summer monsoon to changes in El Niño properties. *Q J Roy Meteor Soc* 131:805–831
- Bellenger H, Guilyardi E, Leloup J, Lengaigne M, Vialard J (2014) ENSO representation in climate models: from CMIP3 to CMIP5. *Clim Dyn* 42:1999–2018
- Boyle JS, Klein SA, Lucas DD, Ma HY, Tannahill J, Xie S (2015) The parametric sensitivity of CAM5's MJO. *J Geophys Res-Atmos* 120:1424–1444
- Brown JR, Moise AF, Delage FP (2012) Changes in the South Pacific Convergence Zone in IPCC AR4 future climate projections. *Clim Dyn* 39:1–19
- Brown JR, Moise AF, Colman RA (2013) The South Pacific Convergence Zone in CMIP5 simulations of historical and future climate. *Clim Dyn* 41:2179–2197
- Brown SJ, Murphy JM, Sexton DMH, Harris GR (2014) Climate projections of future extreme events accounting for modelling uncertainties and historical simulation biases. *Clim Dyn* 43:2681–2705
- Choi KY, Vecchi GA, Wittenberg AT (2015) Nonlinear zonal wind response to ENSO in the CMIP5 models: roles of the zonal and meridional shift of the ITCZ/SPCZ and the simulated climatological precipitation. *J Clim* 28:8556–8573
- Chung CTY, Power SB (2015) Modelled rainfall response to strong El Niño sea surface temperature anomalies in the tropical Pacific. *J Clim* 28:3133–3151
- Clarke A (2008) An introduction to the dynamics of El Niño and the Southern Oscillation. Academic Press 324 pp
- Collins M, Booth BB, Bhaskaran B, Harris GR, Murphy JM, Sexton DMH, Webb MJ (2011) Climate model errors, feedbacks and forcings: a comparison of perturbed physics and multi-model ensembles. *Clim Dyn* 36:1737–1766
- Cubasch U et al (2001) Projections of future climate change, Chapter 9. In: Houghton et al. (eds) *Climate change 2001: The scientific basis, third assessment report of the intergovernmental panel on climate change* JT. Cambridge University Press, Cambridge, New York, pp 525–582
- Dai N, Arkin PA (2017) Twentieth century ENSO-related precipitation mean states in twentieth century reanalysis, reconstructed precipitation and CMIP5 models. *Climate Dynamics* 48 (9–10):3061–3083
- Gilmore MS, Straka JM, Rasmussen EN (2004) Precipitation uncertainty due to variations in precipitation particle parameters within a simple microphysics scheme. *Mon Weather Rev* 132:2610–2627
- Giorgi F, Meams LO (2002) Calculation of average, uncertainty range, and reliability of regional climate changes from AOGCM simulations via the “reliability ensemble averaging” (REA) method. *J Clim* 15:1141–1158
- Gong HN, Wang L, Chen W, Nath D, Huang G, Tao WC (2015) Diverse Influences of ENSO on the East Asian-Western Pacific Winter Climate Tied to Different ENSO Properties in CMIP5 Models. *J Clim* 28:2187–2202

- Große MR et al (2014) Assessment of the CMIP5 global climate model simulations of the western tropical Pacific climate system and comparison to CMIP3. *Int J Climatol* 34:3382–3399
- Guo Z et al (2014) A sensitivity analysis of cloud properties to CLUBB parameters in the single-column Community Atmosphere Model (SCAM5). *J Adv Model Earth Syst* 6:829–858
- Guo Z et al (2015) Parametric behaviors of CLUBB in simulations of low clouds in the Community Atmosphere Model (CAM). *J Adv Model Earth Syst* 7:1005–1025
- Ham YG, Kug JS (2014) ENSO phase-locking to the boreal winter in CMIP3 and CMIP5 models. *Clim Dyn* 43:305–318
- Ham YG, Kug JS (2015) Improvement of ENSO Simulation Based on Intermodel Diversity. *J Clim* 28:998–1015
- Hawkins E, Sutton R (2009) The potential to narrow uncertainty in regional climate predictions. *Bull Am Meteorol Soc* 90:1095
- He SP, Wang HJ (2013) Oscillating relationship between the East Asian winter monsoon and ENSO. *J Clim* 26:9819–9838
- Hou ZS, Huang MY, Leung LR, Lin G, Ricciuto DM (2012) Sensitivity of surface flux simulations to hydrologic parameters based on an uncertainty quantification framework applied to the Community Land Model. *J Geophys Res-Atmos* 117
- Hourdin F et al (2017) The art and science of climate model tuning. *Bull Am Meteorol Soc* 98:589–602
- Huang DQ, Zhu J, Zhang YC, Huang AN (2013) Uncertainties on the simulated summer precipitation over Eastern China from the CMIP5 models. *J Geophys Res-Atmos* 118:9035–9047
- Huang WY et al (2019) A possible mechanism for the occurrence of wintertime extreme precipitation events over South China. *Clim Dyn* 52:2367–2384. <https://doi.org/10.1007/s00382-018-4262-8>
- Hurrell JW et al (2013) The community earth system model a framework for collaborative research. *Bull Am Meteorol Soc* 94:1339–1360
- Jackson CS, Sen MK, Huerta G, Deng Y, Bowman KP (2008) Error Reduction and convergence in climate prediction. *J Clim* 21:6698–6709
- Kang IS et al (2002) Intercomparison of the climatological variations of Asian summer monsoon precipitation simulated by 10 GCMs. *Clim Dyn* 19:383–395
- Kim ST, Cai WJ, Jin FF, Yu JY (2014) ENSO stability in coupled climate models and its association with mean state. *Clim Dyn* 42:3313–3321
- Kug J-S, Ham Y-G, Lee J-Y, Jin F-F (2012) Improved simulation of two types of El Niño in CMIP5 models. *Environ Res Lett* 7:034002. <https://doi.org/10.1088/1748-9326/7/3/034002>
- Lee JY, Wang B (2014) Future change of global monsoon in the CMIP5. *Clim Dyn* 42:101–119
- Li G, Xie SP (2014) Tropical biases in CMIP5 multimodel ensemble: the excessive equatorial Pacific cold tongue and double ITCZ problems. *J Clim* 27:1765–1780
- Li CF et al (2016) Skillful seasonal prediction of Yangtze river valley summer rainfall. *Environ Res Lett* 11
- Li G, Xie S-P, Du Y, Luo Y (2016a) Effects of excessive equatorial cold tongue bias on the projections of tropical Pacific climate change. Part I: the warming pattern in CMIP5 multi-model ensemble. *Climate Dyn* 47:3817–3831
- Li G, Xie S-P, Du Y (2016b) A robust but spurious pattern of climate change in model projections over the tropical Indian Ocean. *J Clim* 29:5589–5608
- Li G, Xie SP, He C, Chen ZS (2017) Western Pacific emergent constraint lowers projected increase in Indian summer monsoon rainfall. *Nat Clim Change* 7:708
- Lindzen RS, Nigam S (1987) On the role of sea-surface temperature-gradients in forcing low-level winds and convergence in the tropics. *J Atmos Sci* 44:2418–2436
- Lintner BR, Langenbrunner B, Neelin JD, Anderson BT, Niznik MJ, Li G, Xie SP (2016) Characterizing CMIP5 model spread in simulated rainfall in the Pacific Intertropical Convergence and South Pacific Convergence Zones. *J Geophys Res-Atmos* 121:11590–11607
- Lopez A, Tebaldi C, New M, Stainforth D, Allen M, Kettleborough J (2006) Two approaches to quantifying uncertainty in global temperature changes. *J Clim* 19:4785–4796
- Lu B, Scaife AA, Dunstone N, Smith D, Ren HL, Liu Y, Eade R (2017) Skillful seasonal predictions of winter precipitation over southern China. *Environ Res Lett* 12
- Mckay MD, Beckman RJ, Conover WJ (1979) A comparison of three methods for selecting values of input variables in the analysis of output from a computer code. *Technometrics* 21:239–245
- McPhaden MJ, Zebiak SE, Glantz MH (2006) ENSO as an integrating concept in Earth science. *Science* 314:1740–1745
- Murphy JM, Booth BB, Boulton CA, Clark RT, Harris GR, Lowe JA, Sexton DMH (2014) Transient climate changes in a perturbed parameter ensemble of emissions-driven earth system model simulations. *Clim Dyn* 43:2855–2885
- Murphy BF, Ye H, Delage F (2015) Impacts of variations in the strength and structure of El Niño events on Pacific rainfall in CMIP5 models. *Clim Dyn* 44:3171–3186
- Neelin JD, Battisti DS, Hirst AC, Jin FF, Wakata Y, Yamagata T, Zebiak SE (1998) ENSO theory. *J Geophys Res-Oceans* 103:14261–14290
- Posselt DJ, Fryxell B, Molod A, Williams B (2016) quantitative sensitivity analysis of physical parameterizations for cases of deep convection in the NASA GEOS-5. *J Clim* 29:455–479
- Qian Y et al (2015) Parametric sensitivity analysis of precipitation at global and local scales in the Community Atmosphere Model CAM5. *J Adv Model Earth Syst* 7:382–411
- Ropelewski CF, Halpert MS (1987) Global and regional scale precipitation patterns associated with the El-Niño southern oscillation. *Mon Weather Rev* 115:1606–1626
- Seager R, Harnik N, Robinson WA, Kushnir Y, Ting M, Huang HP, Veled J (2005) Mechanisms of ENSO-forcing of hemispherically symmetric precipitation variability. *Q J R Meteorol Soc* 131:1501–1527. <https://doi.org/10.1256/qj.04.96>
- Song FF, Zhou TJ (2014a) Interannual variability of East Asian summer monsoon simulated by CMIP3 and CMIP5 AGCMs: skill dependence on Indian Ocean–western Pacific anticyclone teleconnection. *J Clim* 27:1679–1697. <https://doi.org/10.1175/JCLI-D-13-00248.1>
- Song FF, Zhou TJ (2014b) The climatology and interannual variability of east Asian summer monsoon in cmip5 coupled models: does air-sea coupling improve the simulations? *J Clim* 27:8761–8777
- Sperber KR, Palmer TN (1996) Interannual tropical rainfall variability in general circulation model simulations associated with the atmospheric model intercomparison project. *J Clim* 9:2727–2750
- Sperber K et al (2013) The Asian summer monsoon: an intercomparison of CMIP5 vs. CMIP3 simulations of the late 20th century. *Clim Dyn* 41:2711–2744
- Stein M (1987) Large sample properties of simulations using Latin hypercube sampling. *Technometrics* 29:143–151
- Taylor KE, Stouffer RJ, Meehl GA (2012) An overview of Cmp5 and the experiment design. *Bull Am Meteorol Soc* 93:485–498
- Vincent EM, Lengaigne M, Menkes CE, Jourdain NC, Marchesio P, Madec G (2011) Interannual variability of the South Pacific Convergence Zone and implications for tropical cyclone genesis. *Clim Dyn* 36:1881–1896
- Wallace JM, Rasmusson EM, Mitchell TP, Kousky VE, Sarachik ES, von Storch H (1998) The structure and evolution of ENSO-related climate variability in the tropical Pacific: lessons from TOGA. *J Geophys Res-Oceans* 103:14241–14259
- Wang B, Zhang Q (2002) Pacific-east Asian teleconnection. Part II: how the Philippine Sea anomalous anticyclone is established during El Niño development. *J Climate* 15:3252–3265
- Wang B, Wu RG, Fu XH (2000) Pacific-East Asian teleconnection: how does ENSO affect East Asian climate? *J Climate* 13:1517–1536.

- [https://doi.org/10.1175/1520-0442\(2000\)013<1517:Peathd>2.0.Co;2](https://doi.org/10.1175/1520-0442(2000)013<1517:Peathd>2.0.Co;2)
- Wang B, Yang J, Zhou TJ (2008) Interdecadal changes in the major modes of Asian-Australian monsoon variability: strengthening relationship with ENSO since the late 1970s. *J Clim* 21:1771–1789
- Watanabe M et al (2010) Improved climate simulation by MIROC5. Mean states, variability, and climate sensitivity. *J Clim* 23:6312–6335
- Wu RG, Wang B (2002) A contrast of the east Asian summer monsoon-ENSO relationship between 1962–77 and 1978–93. *J Clim* 15:3266–3279
- Wu TW et al (2010) The Beijing Climate Center atmospheric general circulation model: description and its performance for the present-day climate. *Clim Dyn* 34:123–147
- Wu TW et al (2019) The Beijing Climate Center Climate System Model (BCC-CSM): the main progress from CMIP5 to CMIP6. *Geosci Model Dev* 12:1573–1600. <https://doi.org/10.5194/gmd-12-1573-2019>
- Xie PP, Arkin PA (1997) Global precipitation: a 17-year monthly analysis based on gauge observations, satellite estimates, and numerical model outputs. *Bull Am Meteorol Soc* 78:2539–2558
- Xie SP, Hu KM, Hafner J, Tokinaga H, Du Y, Huang G, Sampe T (2009) Indian Ocean capacitor effect on Indo-Western Pacific climate during the summer following El Niño. *J Clim* 22:730–747
- Yan HP et al (2015) A new approach to modeling aerosol effects on East Asian climate: Parametric uncertainties associated with emissions, cloud microphysics, and their interactions. *J Geophys Res-Atmos* 120:8905–8924
- Yang B, Qian Y, Lin G, Leung R, Zhang Y (2012) Some issues in uncertainty quantification and parameter tuning: a case study of convective parameterization scheme in the WRF regional climate model. *Atmos Chem Phys* 12:2409–2427
- Yang B et al (2013) Uncertainty quantification and parameter tuning in the CAM5 Zhang-McFarlane convection scheme and impact of improved convection on the global circulation and climate. *J Geophys Res-Atmos* 118:395–415
- Yang SH, Li CF, Lu RY (2014) Predictability of winter rainfall in South China as demonstrated by the coupled models of ENSEMBLES. *Adv Atmos Sci* 31:779–786
- Yang B, Zhang YC, Qian Y, Huang AN, Yan HP (2015a) Calibration of a convective parameterization scheme in the WRF model and its impact on the simulation of East Asian summer monsoon precipitation. *Clim Dyn* 44:1661–1684
- Yang B, Zhang Y, Qian Y, Wu T, Huang A, Fang Y (2015b) Parametric sensitivity analysis for the Asian summer monsoon precipitation simulation in the Beijing Climate Center AGCM, Version 2.1. *J Climate* 28:5622–5644. <https://doi.org/10.1175/JCLI-D-14-00655.1>
- Yang ZF, Huang WY, Qiu TP, He XS, Wright JS, Wang B (2018) Interannual variation and regime shift of the evaporative moisture sources for wintertime precipitation over southern China. *J Geophys Res* 123:13168–13185. <https://doi.org/10.1029/2018JD029513>
- Yang ZF, Huang WY, He XS, Wang Y, Qiu TP, Wright JS, Wang B (2019) Synoptic conditions and moisture sources for extreme snowfall events over east China. *J Geophys Res* 124:601–623. <https://doi.org/10.1029/2018JD029280>
- Zhang T, Sun DZ (2014) ENSO asymmetry in CMIP5 models. *J Clim* 27:4070–4093
- Zhang MH, Li SL, Lu J, Wu RG (2012) Comparison of the northwestern pacific summer climate simulated by AMIP II AGCMs. *J Clim* 25:6036–6056
- Zhang WJ et al (2016) Unraveling El Niño's impact on the east asian monsoon and Yangtze River summer flooding. *Geophys Res Lett* 43:11375–11382
- Zhao C et al (2013) A sensitivity study of radiative fluxes at the top of atmosphere to cloud-microphysics and aerosol parameters in the community atmosphere model CAM5. *Atmos Chem Phys* 13:10969–10987
- Zhou ZQ, Xie SP, Zheng XT, Liu QY, Wang H (2014) Global warming-induced changes in El Niño teleconnections over the North Pacific and North America. *J Clim* 27:9050–9064. <https://doi.org/10.1175/Jcli-D-14-00254.1>

**Publisher's note** Springer Nature remains neutral with regard to jurisdictional claims in published maps and institutional affiliations.